RESEARCH ARTICLE

QseC Inhibitors as an Antivirulence Approach for Gram-Negative Pathogens

Meredith M. Curtis,[a,b] Regan Russell,[a,b] Cristiano G. Moreira,[a,b*] Adeniyi M. Adebesin,[b,c] Changguang Wang,[b] Noelle S. Williams,[b] Ron Taussig,[c] Don Stewart,[d] Philippe Zimmern,[e] Biao Lu,[b,c] Ravi N. Prasad,[b,c] Chen Zhu,[b,c] David A. Rasko,[f] Jason F. Huntley,[g] John R. Falck,[b,c] Vanessa Sperandio[a,b]

Department of Microbiology,[a] Department of Biochemistry,[b] Department of Pharmacology,[c] and Department of Urology,[e] UT Southwestern Medical Center, Dallas, Texas, USA; Omm Scientific, Dallas, Texas, USA[d]; Department of Microbiology and Immunology and the Institute for Genome Sciences, University of Maryland School of Medicine, Baltimore, Maryland, USA[f]; College of Medicine and Life Sciences, University of Toledo, Toledo, Ohio, USA[g]

* Present address: Cristiano G. Moreira, Biological Sciences Department, School of Pharmaceutical Sciences, São Paulo State University-UNESPAraraquara, São Paulo, Brazil.

M.M.C., R.R., and C.G.M. contributed equally to this work.

ABSTRACT **Invasive pathogens interface with the host and its resident microbiota through interkingdom signaling. The bacterial receptor QseC, which is a membrane-bound histidine sensor kinase, responds to the host stress hormones epinephrine and norepinephrine and the bacterial signal AI-3, integrating interkingdom signaling at the biochemical level. Importantly, the QseC signaling cascade is exploited by many bacterial pathogens to promote virulence. Here, we translated this basic science information into development of a potent small molecule inhibitor of QseC, LED209. Extensive structure activity relationship (SAR) studies revealed that LED209 is a potent prodrug that is highly selective for QseC. Its warhead allosterically modifies lysines in QseC, impairing its function and preventing the activation of the virulence program of several Gram-negative pathogens both *in vitro* and during murine infection. LED209 does not interfere with pathogen growth, possibly leading to a milder evolutionary pressure toward drug resistance. LED209 has desirable pharmacokinetics and does not present toxicity *in vitro* and in rodents. This is a unique antivirulence approach, with a proven broad-spectrum activity against multiple Gram-negative pathogens that cause mammalian infections.**

IMPORTANCE **There is an imminent need for development of novel treatments for infectious diseases, given that one of the biggest challenges to medicine in the foreseeable future is the emergence of microbial antibiotic resistance. Here, we devised a broad-spectrum antivirulence approach targeting a conserved histidine kinase, QseC, in several Gram-negative pathogens that promotes their virulence expression. The LED209 QseC inhibitor has a unique mode of action by acting as a prodrug scaffold to deliver a warhead that allosterically modifies QseC, impeding virulence in several Gram-negative pathogens.**

Received 17 October 2014 **Accepted** 20 October 2014 **Published** 11 November 2014

Citation Curtis MM, Russell R, Moreira CG, Adebesin AM, Wang C, Williams NS, Taussig R, Stewart D, Zimmern P, Lu B, Prasad RN, Zhu C, Rasko DA, Huntley JF, Falck JR, Sperandio V. 2014. QseC inhibitors as an antivirulence approach for Gram-negative pathogens. mBio 5(6):e02165-14. doi:10.1128/mBio.02165-14.

Editor Philippe J. Sansonetti, Pasteur Institute

Address correspondence to Vanessa Sperandio, vanessa.sperandio@utsouthwestern.edu.

This article is a direct contribution from a Fellow of the American Academy of Microbiology.

Antimicrobial resistance poses an alarming threat to public health, with a rising number of infections being refractory to antibiotic treatment. Microorganisms naturally develop drug resistance, and the misuse of antibiotics coupled with the limited development of new antimicrobials has allowed for a surge in the emergence of resistance. Historically, antibiotics were aimed at essential targets and were either bacteriostatic or bactericidal. To combat these emerging resistant populations, as well as the complications that can accompany antibiotic therapy, the next generation of antimicrobial drugs must exploit new therapeutic strategies. One promising approach impedes signaling pathways responsible for expression of virulence traits (1, 2). Inhibitors of virulence are being developed to target a wide range of bacteria (1, 2). The appeal of these antivirulence approaches is that they prevent disease by disrupting the expression of a pathogen's virulence repertoire but do not interfere with growth, possibly engendering a lower evolutionary pressure toward the development of drug resistance (1).

We sought to identify an inhibitor of the bacterial membrane-bound histidine sensor kinase QseC. QseC is an attractive target, as it is present in at least 25 important human and plant pathogens (Fig. 1) and contributes to the virulence of every pathogen examined thus far, including enterohemorrhagic *Escherichia coli* (EHEC) O157:H7, *Salmonella enterica*, uropathogenic *E. coli* (UPEC), nontypeable *Haemophilus influenzae*, *Aeromonas hydrophila*, *Aggregatibacter actinomycetemcomitans*, *Edwardsiella tarda*, and *Francisella tularensis* (3–15). QseC responds to the host stress hormones epinephrine and norepinephrine, as well as to the bacterial signal AI-3 (16). Upon sensing its signals, QseC autophosphorylates and then transfers its phosphate to three response reg-

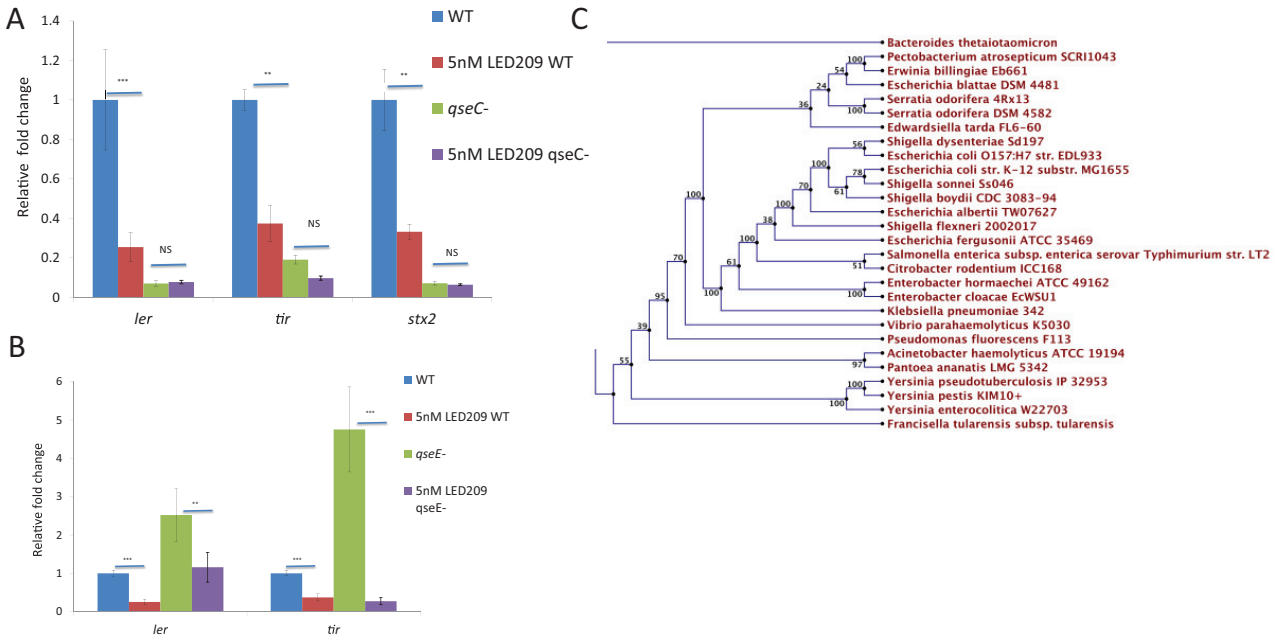

FIG 1 LED209 targets the histidine sensor kinase QseC to attenuate virulence gene expression. (A, B) LED209 signals through the bacterial receptor QseC but not through the bacterial receptor QseE. Wild-type (WT) EHEC and the Δ*qseC* (A) and Δ*qseE* (B) isogenic mutants were grown *in vitro* in the presence (5 nM) or absence (DMSO only) of LED209 to late logarithmic phase. Expression of *ler*, the master transcriptional regulator of the LEE pathogenicity island in EHEC, of *tir*, a key LEE-encoded virulence gene, and of *stx2a*, a subunit of Shiga toxin, was measured by qRT-PCR. Expression is relative to that of the WT grown in the absence of LED209 (error bars, standard deviation [SD]; **, $P < 0.01$; ***, $P < 0.001$; NS, not significant). (C) QseC homologues are present in more than 25 plant and animal pathogens.

ulators (RRs): its cognate RR QseB and the noncognate QseF and KdpE RRs (see Fig. S1 in the supplemental material) (17). Upon phosphorylation, these RRs directly regulate expression of different sets of genes in EHEC. QseB is involved in regulation of the flagella and motility genes (17, 18); KdpE directly activates transcription of the locus of enterocyte effacement (LEE) genes that are key to EHEC virulence (17, 19); QseF is involved in the regulation of the *stxAB* genes encoding Shiga toxin that is responsible for the often-fatal complication hemolytic uremic syndrome (HUS) (17). The broad distribution of QseC among Gram-negative pathogens, and the inherent involvement of this signaling cascade in bacterial pathogenesis, indicates that interference with QseC signaling is a promising strategy to develop broad-spectrum drugs (1, 4).

We previously identified an inhibitor of QseC, LED209 [*N*-phenyl-4-(3-phenylthioureido)benzenesulfonamide], through a high-throughput screen (HTS) of a library of 150,000 small organic compounds and subsequent lead optimization (4). *In vitro* treatment of EHEC, *Salmonella enterica* serovar Typhimurium, and *F. tularensis* with LED209 resulted in a global reduction of virulence traits in a QseC-dependent manner, confirming the suitability of the HTS to identify candidate inhibitors of QseC. Furthermore, administration of LED209 during either *S.* Typhimurium or *F. tularensis* murine infection cogently demonstrated the ability of this scaffold to suppress the pathogenicity of these Gram-negative bacteria (4).

While LED209 emerged as a promising antimicrobial agent during preliminary *in vitro* and *in vivo* studies, many questions remained regarding its mechanism of inhibition of QseC-mediated virulence, its toxicity, its biochemical interaction with QseC, and its efficacy as a broad-spectrum antivirulence drug. Herein, we report that LED209 acts as a prodrug, releasing a selective warhead that interacts potently with QseC via allosteric modification and inactivation. Extensive SAR analysis shows that minor modification of either LED209 or the QseC receptor significantly impacts efficacy. Additionally, we have extended our studies to show that LED209 can function as both a therapy for existing infections and also prophylactically to prevent *S. enterica* and *F. tularensis* murine infections. We also expand the spectrum of Gram-negative pathogens susceptible to LED209 treatment to include multidrug-resistant clinical isolates of UPEC, *Klebsiella*, and *Pseudomonas aeruginosa*. Finally we show that LED209 can decrease biofilm formation by multiple pathogens, including the deadly enteroaggregative *E. coli* (EAEC) O104:H4 responsible for a 2011 outbreak of diarrhea and HUS in Germany.

RESULTS

LED209 acts as a prodrug, allosterically modifying QseC. We have previously reported that LED209 significantly attenuates virulence in the human pathogens EHEC, *Salmonella*, and *F. tularensis* without inhibiting pathogen growth (4). Compounds that interfere with pathogen virulence represent a novel class of antimicrobial drugs that offer an alternative treatment against microbes that are resistant to current antimicrobials. Using QseC reconstituted in liposomes, we showed biochemically that LED209 acted on the QseC receptor, preventing binding to its signals and consequently its autophosphorylation in response to them (4). To further determine the specificity of LED209 to QseC,

we took a genetic approach. We evaluated the expression of key virulence genes after treatment with LED209 *in vitro* in the EHEC wild type (WT) and in isogenic *qseC* and *qseE* mutants. The histidine sensor kinases QseC and QseE positively and negatively regulate virulence gene expression in EHEC, respectively, and QseE also responds to epinephrine as a signal (20). The *qseC* mutant was refractory to treatment with LED209, whereas the *qseE* mutant remained responsive to LED209 treatment, further indicating that LED209 acts through QseC (Fig. 1A and B). Importantly, treatment of the WT with LED209 phenocopied a *qseC* mutation (Fig. 1A). Because QseC phosphorylates three RRs (17), we delved into mapping through which RR LED209-mediated QseC inhibition is decreasing virulence expression in the human pathogen EHEC. We chose to map this circuit in EHEC, because the QseC signaling cascade has been studied in exquisite genetic and biochemical mechanistic detail in this pathogen, with the mode of action of all three response regulators (QseB, KdpE, and QseF) being defined (16–29). As expected, expression of the virulence genes was decreased in a Δ*qseBC* mutant (see Fig. S1B in the supplemental material), and this mutant did not respond to LED209, similarly to the Δ*qseC* mutant (Fig. 1A). QseC-dependent expression of the virulence genes (LEE) occurs through the KdpE RR (17, 19), and concurrent with previous reports, expression of these genes was decreased in the Δ*kdpE* mutant, which is also nonresponsive to LED209 and phenocopies the LED209 decreased virulence gene expression in the WT (see Fig. S1), akin to the phenotype of the Δ*qseC* mutant (Fig. 1A) (11, 12, 17, 30). It is noteworthy that when using animal models, Δ*qseC*, Δ*qseBC*, and Δ*kdpE* mutants are all attenuated for infection (see Fig. S1). QseC homologues are present in more than 25 plant and animal pathogens, suggesting that QseC inhibitors might have broad effectiveness against Gram-negative pathogens (Fig. 1C).

Because of the high conservation of QseC across numerous bacterial species, we sought to better understand the mechanism by which LED209 inhibited QseC, as LED209 represents a potential broad-spectrum therapeutic. LED209 acts as a prodrug, and upon interaction of LED209 with its target QseC within the bacterial cell, it acts as a prodrug by loss of an aniline group to release the warhead of LED209, isothiocyanate OM188 (Fig. 2A). The delivery of OM188 via LED209 avoids the metabolism and/or degradation experienced by OM188 en route to the target. It is worth noting that conversion of LED209 to OM188 via cleavage of the aniline occurs only within the bacterial cell and presumably in close proximity to QseC. This would help account for the remarkable potency of LED209. We cannot detect OM188 or the cleaved aniline in mammalian tissues (data set available from the author). This is a bacterium-specific hydrolysis of the prodrug, which alleviates concerns of host toxicity, which our toxicity studies described below confirm to be negative. Treatment of EHEC with 500 nM of OM188 significantly reduced the expression of the EHEC *ler* gene that encodes a transcriptional regulator that activates expression of key virulence genes responsible for the EHEC-mediated hemolytic colitis, the *eae* gene encoding an essential adhesin to establish gut colonization, and the gene (*stx2a*) encoding the Shiga toxin that leads to HUS following EHEC infections (Fig. 2B). Additionally, treatment with OM188 also reduced the formation of attaching and effacing (A/E) lesions, a hallmark of EHEC infection and a requisite for gut colonization and diarrheal disease (Fig. 2C and D). Moreover, OM188 also decreased *Salmonella enterica* serovar Typhimurium intramacrophage replication (Fig. 2E), which is also a QseC-dependent virulence phenotype inhibited by LED209 (see Fig. 5D).

An azide was added to OM188 to perform click chemistry, generating OM201. We determined that OM201 directly binds to QseC (Fig. 3A and B) and that OM201 is still active to decrease virulence gene expression (Fig. 2C). Mass spectrometry analysis confirmed that OM188 directly binds to two lysine residues (K256 and K427) on QseC (Fig. 3D). Importantly, K256 is conserved in the QseC from all *E. coli* strains, including EHEC, and from *Salmonella enterica*, *Shigella* species, *Citrobacter rodentium*, *Enterobacter* species, *Klebsiella pneumoniae*, *Erwinia* species, *Pectobacterium atrosepticum*, and *F. tularensis* (Fig. 3E). K427 is conserved only in *E. coli* and *Shigella* species (Fig. 3E). We generated site-directed mutants of QseC in both K256 and K427, changing K to R to assess the role of these lysines in QseC function (strains RR03 and RR04). Both QseC mutant proteins were expressed normally and folded properly (data not shown). However, neither mutant was able to activate expression of the EHEC virulence genes (Fig. 3F), suggesting that modification of either of these lysines impairs QseC function, akin to the block observed by treatment with LED209 or its warhead OM188 (Fig. 1 and 2).

SAR of LED209 shows that minor structural modifications significantly impact its activity. An extensive SAR of LED209 (see Table S6 in the supplemental material) was conducted and, for simplicity, the structure of LED209 was divided into four major regions (Fig. 4A). Modifications to the left-hand aniline group (part A) abolished the bioactivity of LED209 (Fig. 4B). Treatment with CF290 resulted in a 2-fold increase of *ler*, reversing the strong antagonist activity of LED209 into a slight agonist of EHEC virulence. CF287 also lost the antagonist activity seen with LED209 and returned expression levels of *ler* and *stx2a* to those seen in the untreated control group. Alterations to part A likely disrupt LED209's ability to act as a prodrug and release its active component OM188. Modifications to part C, as exemplified in compound CF252, also reversed the antagonist behavior of LED209. In contrast, replacing the benzene ring located in part D with a cyclohexane (CF283) did not modify the antagonist activity compared with the parent LED209. CF283 significantly reduced the expression of both *ler* and *stx2a* (Fig. 4B).

A commercially available version of LED209 (Sigma-Aldrich), sold as LED209 hydrate, was devoid of LED209-like antagonist activity against EHEC. Treatment with LED209 hydrate (Sigma LED209) did not alter virulence gene expression levels compared with those of the untreated control (Fig. 4C) and also failed to decrease A/E lesion formation (Fig. 4D and E). The origins of the problems with the Sigma-Aldrich material were further investigated (data set available from the author) and showed that the Sigma-Aldrich LED209 product did not contain LED209 but rather a mixture of CF104 and OM124 (sample B in the data set; all other samples are different batches of LED209 synthesized by us), which are both inactive compounds (see Table S6 in the supplemental material). To provide consistency for future studies, a large-scale batch of LED209 was manufactured according to Good Laboratory Practice (GLP) regulations, and it works as well as all of our previous LED209 batches to block bacterial virulence expression (Fig. 4F).

Treatment with LED209 protects against *S.* Typhimurium and *F. tularensis* murine infections. *Salmonella enterica* serovar Typhimurium carries a homolog of the EHEC QseC (87% similarity). QseC acts globally in *S.* Typhimurium to regulate key vir-

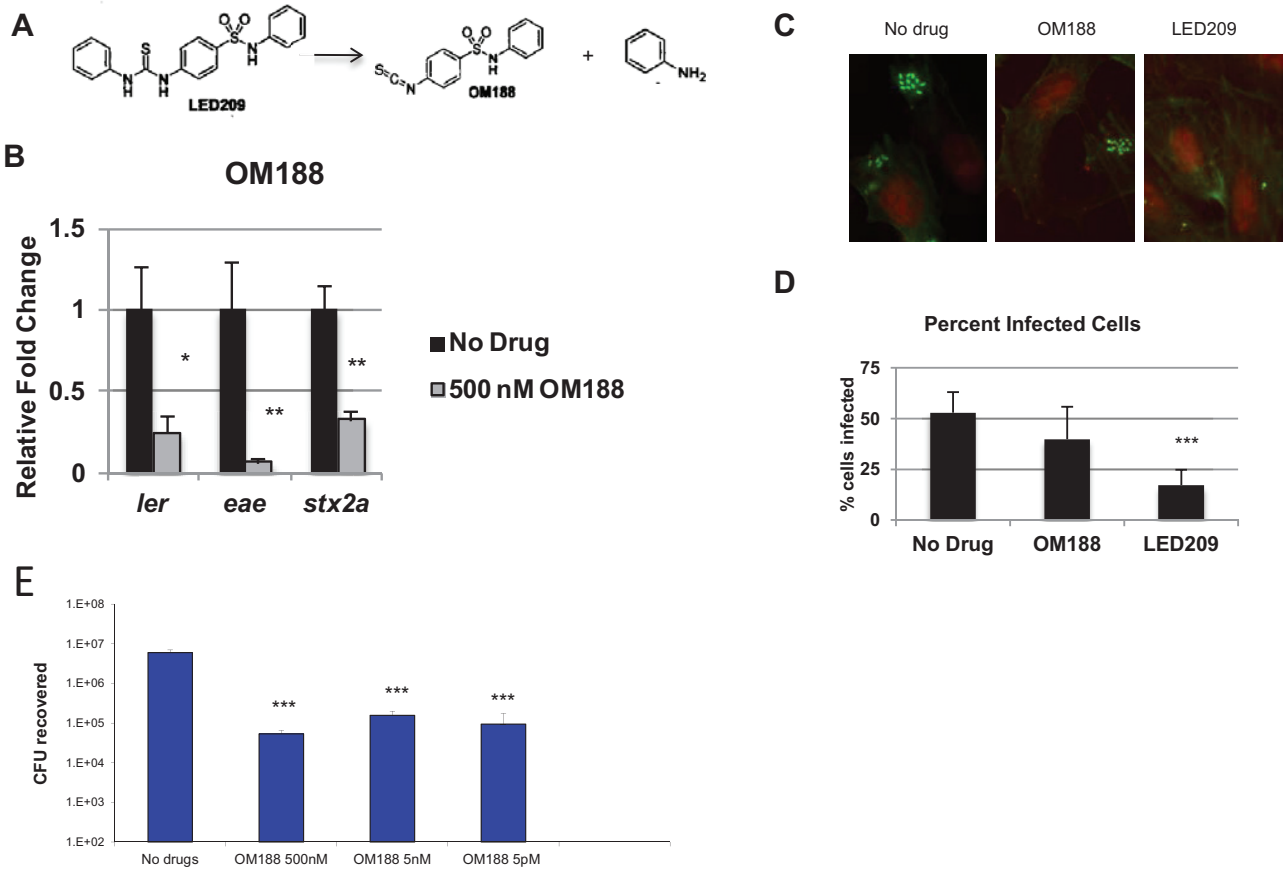

FIG 2 LED209 acts as a prodrug, cleaving an aniline group to expose its active component. (A) Upon interaction with QseC, LED209 breaks into the active component of LED209, OM188, and an aniline group. Schematic depicts the breakdown of LED209. OM188 contains an isothiocyanate (S=C=N) that is reactive to lysine and cysteine. (B) Treatment of EHEC with OM188 *in vitro* (by adding DMSO to the no-drug control and OM188 in DMSO at the beginning of the experiment) decreases expression of virulence genes. WT EHEC was grown *in vitro* in the presence (500 nM) or absence (DMSO only) of OM188 to late logarithmic phase. Expression of *ler*, *eae*, and *stx2a* was measured by qRT-PCR. Expression is relative to that of the WT grown in the absence of OM188 (error bars, SD; **, $P < 0.01$; *, $P < 0.05$). (C) Fluorescent actin staining assay of HeLa cells infected with EHEC grown in the absence (DMSO, no drug) or presence (5 nM) of OM188 or LED209, stained with fluorescein isothiocyanate-phalloidin (actin, green) and propidium iodide (bacterial and HeLa DNA, red). Original magnification, ×63. (D) Quantification of fluorescent actin staining assay of the percentage of HeLa cells infected, as defined by pedestal formation by EHEC ($n = 100$ cells). (E) Intramacrophage replication of *S. enterica* Typhimurium in the presence and absence of OM188 (error bars, SD; ***, $P < 0.001$; **, $P < 0.01$; *, $P < 0.05$).

ulence genes required for flagellar motility, invasion of epithelial cells, survival within macrophages, and murine infection, with the *qseC* mutant being nonvirulent in mice (4, 8, 31). A single dose of LED209 (20 mg/kg of body weight) or a vehicle control was administered orally to mice 30 min prior to intraperitoneal injection of a lethal dose of *S.* Typhimurium. Seventy-two hours after infection, 25% of the untreated mice remained alive, whereas 60% of the LED209-treated group remained alive (Fig. 5A). Twenty-five percent of the untreated mice survived up to 6 days after infection, while 50% of the LED209-treated group survived up to 6 days after infection. To determine if a more rigorous dosing regimen would increase protection against *S.* Typhimurium infection, LED209 (20 mg/kg) was administered at 3 h before, at the time of, and 3, 6, 9, and 12 h after intraperitoneal injection of a lethal dose of *S.* Typhimurium. At 48 h, only 14% of the untreated mice remained alive, with none surviving beyond 72 h postinfection, whereas 43% of the LED209-treated mice remained alive and survived up to 8 days after infection, when these animals were sacrificed (Fig. 5B). Expression of *sifA*, an effector secreted via the type III secretion system SPI-2 and required for vacuolar replication, was significantly decreased when LED209 was administered during *in vitro* growth in minimal medium (Fig. 5C). The addition of LED209 also decreased survival of *S.* Typhimurium within macrophages by 4 logs (Fig. 5D).

F. tularensis also encodes a homolog of the EHEC QseC (57% similarity) that serves as the sole histidine sensor kinase encoded within the *F. tularensis* genome. We previously demonstrated that LED209 treatment decreases the expression of several *F. tularensis* virulence genes and markedly decreases macrophage survival *in vitro*. To explore the dosing requirements to yield protection against a lethal dose of intranasal *F. tularensis*, a single dose of LED209 was administered orally to mice either 1, 3, 6, 9, or 24 h prior to infection or alternatively 1, 3, 6, 9, or 24 h after infection (Fig. 5E and F). Pretreatment with LED209 prior to *F. tularensis* infection provided some protection at the 24-h time point, with 25% of the untreated animals surviving by day 7, while 85% of the

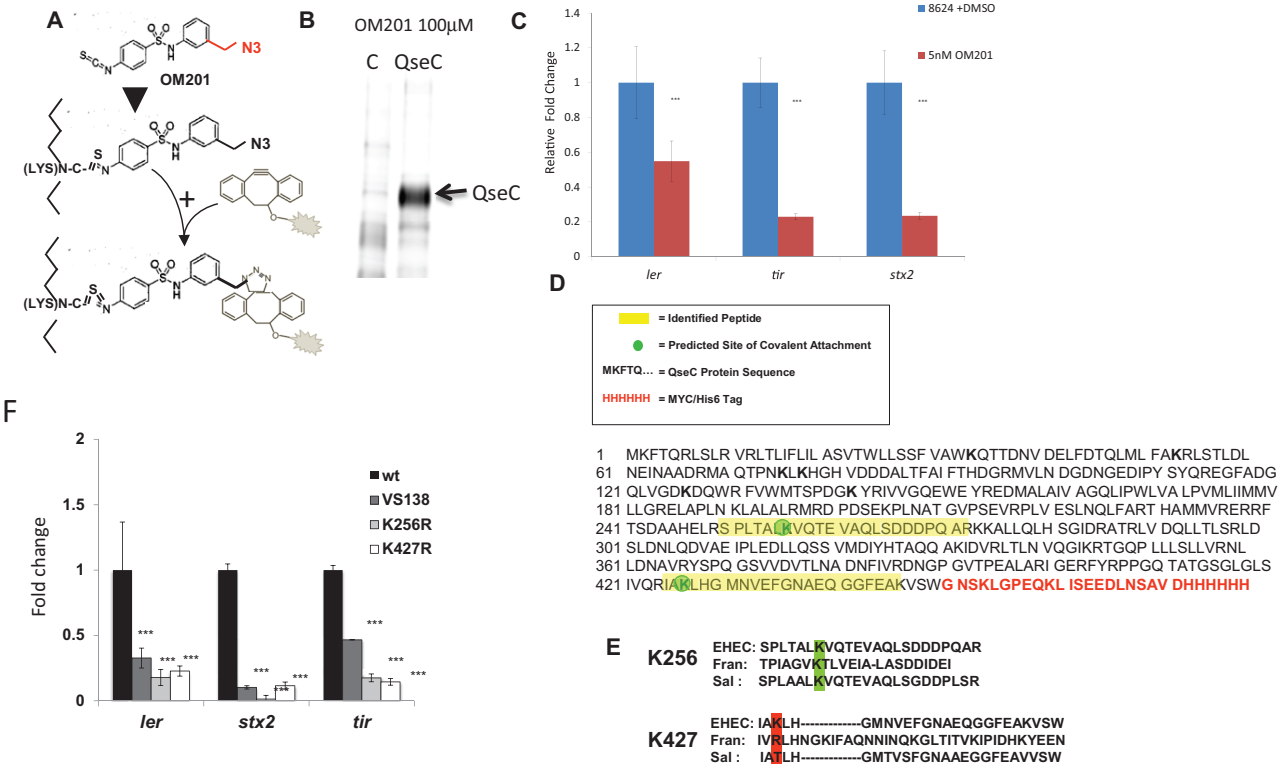

FIG 3 LED209 targets the sensor kinase QseC on a conserved lysine residue. (A) Schematic of the "click chemistry" approach used to identify the conserved lysine residue to which QseC binds. The warhead of LED209, OM188, was engineered to contain an azide group that will "click" with a fluorophore alkyne-containing group. The "click" compound was named OM201. (B) OM201 binds to QseC *in vitro*. Membrane preparations of the Δ*qseC* mutant with empty vector (C [no QseC]) or expressing QseC (pVS155) were incubated with 100 μM OM201 and then run on an SDS-PAGE gel to separate proteins. (C) qRT-PCR of EHEC virulence genes (*ler*, *tir*, and stx_2) in the absence or presence of OM201 (5 nM) showing that OM201 is active to inhibit virulence gene expression. (D) Two conserved lysine residues were identified through mass spectrometric analysis as candidates to covalently bind to OM188. Membrane preparations preincubated with OM188 were submitted for peptide analysis by LC-MS. Peptide fragments containing lysine 256 (K256) and lysine 427 (K427) were bound to OM188 and predicted to be sites of covalent attachment. (E) Alignment of QseC peptide sequences in EHEC, *S.* Typhimurium, and *F. tularensis* indicates that K256 is conserved in all three species. (F) Mutation of conserved lysines K256 and K427 result in a loss of virulence. qRT-PCR of the expression of the EHEC virulence genes: *ler* encodes a transcriptional activator of virulence genes, *tir* encodes a key virulence factor, and stx_2 encodes the Shiga toxin in the Δ*qseC* (VS138) with *qseC* WT (pVS155), Δ*qseC* (VS138), Δ*qseC* (VS138) with the K256R or K427R *qseC* mutants. ***, $P < 0.001$.

treated animals were alive. By day 8, 10% of the untreated animals and 50% of the treatment animals were alive. In contrast, a single dose of LED209 administered at 3 or 6 h after infection provided more significant protection compared to that of the untreated mice. On day 7 after infection, 85% of the mice treated at 3 h postinfection, 75% of the mice treated at 6 h postinfection, and 85% of the mice treated 24 h postinfection remained alive, while only 20% of the untreated mice remained alive. On day 8, 85% of the mice treated at 3 h, 60% of the mice treated at 6 h, and 60% of the mice treated at 24 h survived, while only 20% of the untreated animals remained alive. On day 9, 80% of the mice treated at 3 h, 50% of the mice treated at 6 h, and 40% of the mice treated at 24 h survived, while only 10% of the untreated animals were alive. Only 10% of the untreated mice survived 12 days postinfection, whereas 80% and 50% of the mice treated at 3 or 6 h postinfection, respectively, survived. The animals that survived were sacrificed at day 12.

LED209 decreases biofilm formation in EAEC O104:H4 and in several multidrug-resistant clinical isolates of rUTIs. The addition of 5 nM LED209 significantly reduced biofilm formation by the enteroaggregative *E. coli* (EAEC) O104:H4 strain isolated during the German outbreak of 2011 (37% reduction; ***, $P = 0.0006$) and by the uropathogenic *E. coli* (UPEC) strain UTI89 (35% reduction; *, $P = 0.0486$); however, LED209 did not significantly reduce biofilm formation by the UPEC strain CFT073 (8% reduction; $P = 0.2682$) (Fig. 6A). Additionally, treatment with LED209 significantly reduced the expression of *stx2a* in EAEC O104:H4 (Fig. 6B). This EAEC Stx-positive strain was responsible for a diarrhea and uremic syndrome outbreak in Germany in 2011 that led to serious morbidity and mortality rates (32). Multidrug-resistant clinical isolates from patients with recurrent urinary tract infections (rUTI) were collected and isolated from urine and bladder biopsy specimens, and the samples were characterized to determine their probable species. The addition of LED209 significantly reduced biofilm formation by several of the isolates. UPEC isolates 6, 8, and 25 achieved reductions of 43%, 48%, and 43% in biofilm formation, respectively (Fig. 6C and D). Furthermore, LED209 proved efficacious against *Pseudomonas* and *Klebsiella* isolates, reducing biofilm formation by 26% in isolate 18 and by 21% in isolate 20 (Fig. 6C and D).

Toxicology and pharmacokinetics of LED209. Our preliminary toxicology studies were performed by treating mice daily

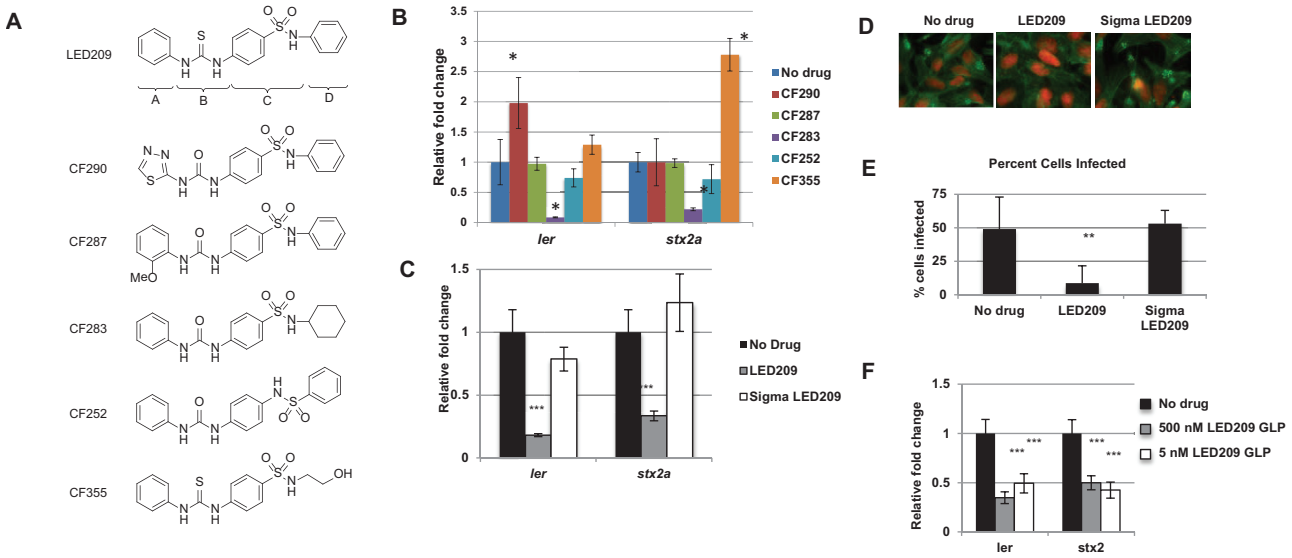

FIG 4 Minor modifications to the structure of LED209 significantly impact its activity. (A) Four major components of LED209: the left-hand aniline group (part A), the thiourea (part B), the sulfur dioxide and amine group (part C), and the right-hand benzene (part D) were modified for structure analysis relationship (SAR) studies. Structures of the modified compounds are depicted in panel A. (B) Modifications to LED209 impact its ability to attenuate virulence gene expression in EHEC. WT EHEC was grown *in vitro* in the presence (5 nM) or absence (DMSO only) of modified compounds to late logarithmic phase. Expression of *ler* and *stx2a* was measured by qRT-PCR. Expression is relative to WT grown in the absence of drug (error bars, SD; *, $P < 0.01$). (C) Commercially available LED209 (Sigma) loses its efficacy with the addition of a hydrate at an undisclosed location. WT EHEC was grown in the presence (5 nM) of either LED209 synthesized at UT Southwestern or LED209 hydrate commercially available through Sigma-Aldrich, and expression of *ler* and *stx2a* was measured by qRT-PCR. Expression is relative to WT grown in the absence of drug (error bars, SD; ***, $P < 0.001$). (D) Fluorescent actin staining assay of HeLa cells infected with EHEC grown in the absence (DMSO, no drug) or presence (5 nM) of LED209 or LED209 hydrate (Sigma), stained with fluorescein isothiocyanate-phalloidin (actin, green) and propidium iodide (bacterial and HeLa DNA, red). Original magnification, ×63. (E) Quantification of fluorescent actin staining assay of the percentage of HeLa cells infected, as defined by pedestal formation by EHEC ($n = 100$ cells; error bars, SD; **, $P < 0.01$). (F) LED209 manufactured according to Good Laboratory Practice (GLP) standards was tested for its ability to inhibit EHEC virulence gene expression. WT EHEC was grown in the presence or absence of LED209 GLP, and expression of *ler* and *stx2a* was measured by qRT-PCR. Expression is relative to WT grown in the absence of drug (error bars, SD; ***, $P < 0.001$).

with 5, 20, and 80 mg/kg of LED209 for 14 days. These studies suggested that LED209 did not present any toxicity, with treated and untreated animals having similar body weights, blood chemistry, complete blood counts (CBC), and levels of T4 (as a measure of thyroid function) and no liver toxicity (see Table S2 to S5 and Fig. S2 in the supplemental material). No effects of LED209 in the hERG channel (see Tables S2 to S5 and Fig. S2 to S4) were observed as measured by a radioligand binding assay in which 10 μM LED209 was tested in duplicate for its ability to block the interaction of 1.5 nM astemizole to the hERG channel expressed recombinantly in HEK293 cells. Minimal inhibition of binding (4%) was observed. An analysis of LED209 plasma levels after oral gavage revealed that the compound shows good oral bioavailability but nonlinear pharmacokinetics by this route (see Fig. S3). Plasma area under the concentration-time curve (AUC_{last}, which is defined as the area under the concentration-time curve from time 0 up to the last measurable concentration) increased more than proportionally with doses from 5 to 80 mg/kg, possibly due to inhibition of drug efflux pumps in the gastrointestinal tract or inhibition of drug metabolism enzyme in the gut or liver at high drug concentrations. Exposures at doses above 80 mg/kg increased less than proportionally with dose. We found that at these higher doses, absorption was incomplete, and a significant amount of compound was simply excreted unchanged in feces. In contrast, LED209 pharmacokinetics via the intravenous route from 5 to 20 mg/kg is linear (4). Despite a relatively short terminal half-life of 40 to 100 min in mice, LED209 showed high peak concentrations in plasma at each dose, which may serve as an efficient means of delivering large amounts of compound into bacterial cells for generation of the active OM188 warhead. Although plasma exposures with LED209 were high, limited penetration of the blood-brain barrier was observed (see Fig. S4).

DISCUSSION

The originality and benefits of the proposed approach to combat infectious diseases are 2-fold. First, this is a broad-spectrum therapeutic antivirulence approach. Most antivirulence approaches are restricted to a specific pathogen. In contrast, the broad distribution of QseC among Gram-negative pathogens, and the inherent involvement of this signaling cascade in bacterial pathogenesis, indicates that interference with QseC signaling is a promising strategy to develop broad-spectrum drugs (1). Second, pathogens sense host neurotransmitters to modulate their virulence gene expression to ensure optimal host colonization. Furthermore, this is also a means for the invading pathogen to gauge the physiological and immunological state of the host. Since these processes do not control bacterial growth, interference with this signaling will only stop virulence, not kill the bacteria. Consequently, this antivirulence approach may engender a lower evolutionary pressure toward the development of drug resistance.

This antivirulence strategy addresses an urgent unmet need in health care. It is clear that we are in a postantibiotic era, with a rapidly contracting armamentarium to combat infectious diseases. Emergence and reemergence of pathogens and antibiotic

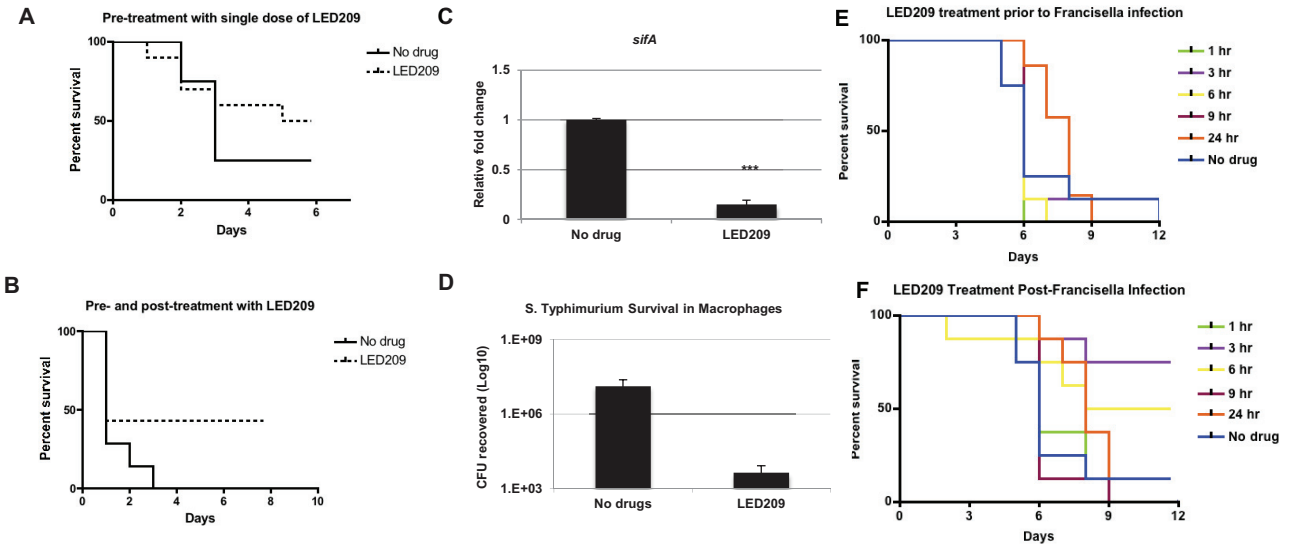

FIG 5 Treatment of LED209 protects against *S.* Typhimurium and *F. tularensis*. (A, B) Administration of LED209 protects BALB/c mice from *S.* Typhimurium infection. Mice were administered a single dose of LED209 (20 mg/kg) at 3 h before (A) or multiple doses of LED209 (20 mg/kg) at 3 h before, at the time of, and 3, 6, 9, and 12 h after (B) intraperitoneal injection of a lethal dose of *S.* Typhimurium (10^6 CFU). Graphs indicate survival to infection ($n = 10$). (C) Treatment of *S.* Typhimurium with 50 nM LED209 *in vitro* decreased the expression of *sifA*, an effector required for vacuolar replication. qRT-PCR of *sifA* in *S.* Typhimurium grown in N-minimal medium to late logarithmic phase. Expression is relative to *S.* Typhimurium grown in the absence of drug (error bars, SD; ***, $P < 0.001$). (D) J774 murine macrophages were infected with opsonized *S.* Typhimurium in the presence (5 nM) or absence (DMSO only) of LED209. Graph indicates intracellular survival within macrophages. (E, F) Administration of LED209 postinfection protects C3H/HeN mice from *F. tularensis* infection. Mice were administered a single dose of LED209 (20 mg/kg) at 1, 3, 6, 9, or 24 h prior to infection and then intranasally infected with 30 CFU of *F. tularensis* strain SCHU S4 (E) or a single dose at 1, 3, 6, 9, or 24 h postinfection with 30 CFU of *F. tularensis* (F). Graphs indicate survival to infection ($n = 10$).

resistance in these "superbugs" have brought infectious diseases to the forefront of global health challenges in the 21st century. However, as promising as these antivirulence approaches are, they come with a new set of regulatory and preclinical development challenges. Pharmaceutical companies and regulatory government agencies are accustomed to relying on MICs or other simple tests for bactericidal or bacteriostatic drugs. Antivirulence drugs require more involved and state-of-the-art testing, often utilizing multiple molecular biology and microbiology techniques to assess whether these drugs are indeed preventing virulence instead of simply killing the pathogens. One can also foresee some potential advantages for these types of approaches; e.g., in addition to treating a bacterial infection, host exposure to a disarmed pathogen may engender immunological protection to recurrent infections, akin to a vaccination approach. Additionally, one can also conceive of combinatorial treatments combining antivirulence and antibiotic strategies, which may extend the clinical utility of several antibiotics.

MATERIALS AND METHODS

Synthesis of compounds. LED209 was synthesized as previously described (4). GLP synthesis of 1 kg of LED209 was conducted by Symmetry Biosciences. LED209 hydrate (L8919) was purchased from Sigma.

OM188. To a stirring, room temperature solution of 4-amino-*N*-phenyl-benzenesulfonamide (4) (CF103; 506 mg, 2.04 mmol) was dissolved in dry tetrahydrofuran (THF; 10 ml), 1,1′-thiocarbonyldiimidazole (484 mg, 90%, 2.44 mmol). After 4.5 h, the THF was removed *in vacuo*, and the residual oil was purified on silica gel (20 to 30% EtOAc-hexanes) to give 475 mg (80%) of isothiocyanate OM188 as a white solid.

***N*-(4-(3-Phenylureido)phenyl)benzenesulfonamide (CF252).** A mixture of *N*-(4-aminophenyl)benzenesulfonamide (80 mg, 0.322 mmol), phenylisocyanate (38.4 mg, 35 μl, 1 equivalent), and triethylamine (NEt_3, 65.2 mg, 90 μl, 2 equivalents) in THF (2 ml) was heated at 60°C. After 12 h, all volatiles were removed *in vacuo*, and the residue was purified by preparative TLC (EtOAc-hexanes, 1:1, 2 elutions) to give CF252 (44 mg, 37%). ^{1}H NMR (300 Mz, CD_3COCD_3) δ 8.78 (br s, 1 H), 8.12 (br s, 2 H), 7.77 to 7.42 (m, 2 H), 7.60 to 7.49 (m, 5 H), 7.42 (d, $J = 9.0$ Hz, 2 H), 7.26 (t, $J = 7.2$ Hz, 1 H), 7.09 (d, $J = 8.7$ Hz, 2 H), 6.99 (t, $J = 7.2$ Hz, 1 H); ^{13}C NMR (100 MHz, CD_3COCD_3) δ 152.42, 139.96, 139.87, 137.32, 132.57, 131.71, 128.88(2), 128.63(2), 127.03(2), 122.78(2), 122.05, 119.06(2), 118.52(2).

***N*-Cyclohexyl-4-(3-phenylureido)benzenesulfonamide (CF283).** Cyclohexylamine (14 mg, 0.142 mmol) and Et_3N (22 μl, 0.155 mmol) were added to a 0°C solution of 4-(3-phenylureido)benzene-1-sulfonyl chloride (40 mg, 0.129 mmol) in dry dichloromethane (2 ml). After being stirred overnight, the mixture was poured into water (10 ml) and extracted with EtOAc (5 ml; three times). The combined organic extracts were washed with brine (5 ml), dried, and concentrated. The residue was purified by PTLC (polar thin-layer chromatography) (CH_2Cl_2-MeOH, 95:5) to give CF283 (40 mg, 83% yield) as a white solid. ^{1}H NMR (300 MHz, CD_3COCD_3) δ 8.66 (br s, 1 H), 8.39 (s, 1 H), 7.79 to 7.69 (m, 4 H), 7.57 to 7.54 (m, 2 H), 7.31 to 7.22 (m, 2 H), 7.03 to 6.98 (m, 1 H), 6.28 (d, $J = 7.5$ Hz, 1 H), 3.16 to 3.00 (m, 1 H), 1.73 to 1.63 (m, 4 H), 1.29 to 1.14 (m, 6 H); ^{13}C NMR (100 MHz, CD_3COCD_3) δ 152.12, 143.54, 139.54, 135.27, 128.69(2), 127.79(2), 122.42, 118.72(2), 117.67(2), 52.45, 33.62(2), 25.10(2), 24.66.

4-(3-(2-Methoxyphenyl)ureido)-*N*-phenylbenzenesulfonamide (CF287). 4-Amino-*N*-phenylbenzenesulfonamide (248 mg, 1.0 mmol) was added to a solution of triphosgene (312 mg, 1.05 mmol) in dry dioxane (4 ml) at room temperature. The reaction mixture was heated at 70°C for 4 h and then concentrated *in vacuo* to give crude 4-isocyanato-*N*-phenylbenzenesulfonamide, which was used without further purification.

2-Methoxyaniline (22 mg, 1 equivalent) was added to a solution of 4-isocyanato-*N*-phenylbenzenesulfonamide in dry THF (1 ml, 50 mg/1 ml). The mixture was heated at 80°C overnight and then concentrated *in*

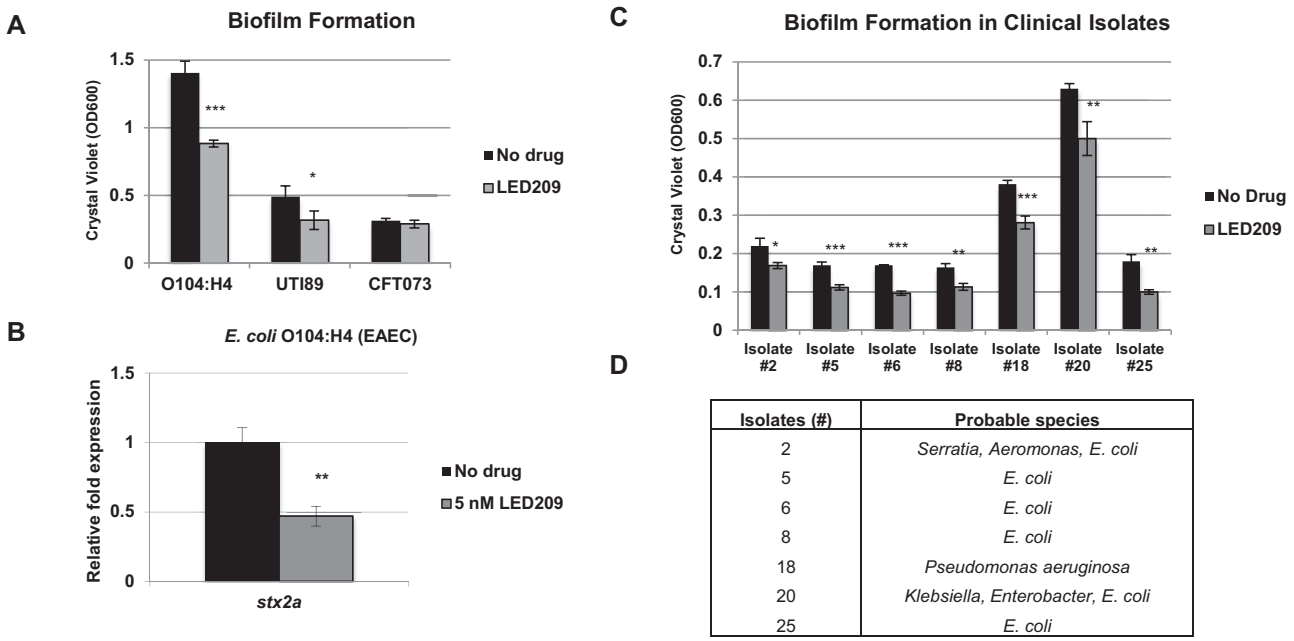

Isolates (#)	Probable species
2	*Serratia, Aeromonas, E. coli*
5	*E. coli*
6	*E. coli*
8	*E. coli*
18	*Pseudomonas aeruginosa*
20	*Klebsiella, Enterobacter, E. coli*
25	*E. coli*

FIG 6 LED209 diminishes biofilm formation in EAEC O104:H4 and in clinical isolates. (A) Treatment with LED209 reduced biofilm formation in the EAEC O104:H4 strain isolated from the 2011 German outbreak and in the UPEC strain UTI89. EAEC O104:H4, UTI89, and CFT073 were grown statically in LB in 96-well plates for 24 h in the presence (5 nM) or absence (DMSO only) of LED209. Biofilm formation was determined by measuring crystal violet binding at OD_{600} following gentle washing to remove unattached bacteria. (B) Treatment with LED209 reduced expression of *stx2a*, a subunit of Shiga toxin, in EAEC O104:H4. EAEC O104:H4 was grown in the presence (5 nM) or absence (DMSO) of LED209 to late logarithmic phase. Expression is relative to EAEC in the absence of drug. (C) Administration of LED209 diminished biofilm formation in clinical isolates isolated from urine and bladder biopsy samples. The isolates were grown statically in LB as described above, and biofilm formation was determined by measuring crystal violet binding at OD_{600} (error bars, SD; ***, $P < 0.001$; **, $P < 0.01$; *, $P < 0.05$). (D) Clinical samples were enriched in LB broth and isolated in MacConkey agar to differentiate Gram-negative bacteria. Isolates were classified via API 20E kits (bioMérieux, France). Probable species include *Pseudomonas*, *Klebsiella*, and *Enterobacter* species.

vacuo. The residue was purified by PTLC (CH_2Cl_2-MeOH, 9:1) to give CF287 (70 mg, 93% yield) as a white solid. ^{1}H NMR (300 MHz, CD_3COCD_3) δ 9.26 (br s, 1 H), 8.89 (br, 1 H), 8.16 to 8.13 (m, 1 H), 8.07 (br, 1 H), 7.69 to 7.65 (m, 4 H), 7.49 to 7.46 (m, 1 H), 7.28 to 7.23 (m, 5 H), 7.08 to 7.03 (m, 2 H), 2.73 (s, 3 H); ^{13}C NMR (100 MHz, CD_3COCD_3) δ 151.83, 147.93, 144.24, 138.12, 132.39, 129.01(2), 128.57, 128.29(2), 124.22, 122.27, 120.63(2), 120.61, 118.61, 117.42(2), 110.30, 55.29.

4-(3-(1,3,4-Thiadiazol-2-yl)ureido)-*N*-phenylbenzenesulfonamide (CF290). Following the above-given procedure, an equimolar mixture of 4-isocyanato-*N*-phenylbenzenesulfonamide and 1,3,4-thiadiazol-2-amine in dry THF (1 ml, 50 mg/1 ml) was heated at 80°C overnight and then concentrated *in vacuo*. Purification of the residue via PTLC gave CF290 (90%) as a white solid. ^{1}H NMR (300 MHz, CD_3SOCD_3) δ 10.2 (s, 1 H), 9.58 (br s, 2 H), 9.04 (br s, 1 H), 7.69 to 7.60 (m, 4 H), 7.23 to 7.18 (m, 2 H), 7.08 to 6.97 (m, 3 H); ^{13}C NMR (100 MHz, CD_3SOCD_3) δ 160.33, 152.29, 148.03, 142.70, 137.83, 132.80, 129.13(2), 128.12(2), 124.00, 120.09(2), 118.16(2).

Synthesis of *N*-(2-hydroxyethyl)-4-(3-phenylthioureido)benzenesulfonamide (CF355). A mixture of *N*-(2-hydroxyethyl)-4-nitrobenzenesulfonamide (530 mg, 2.15 mmol) and 5% WT Pd/C (53 mg) in anhydrous tetrahydrofuran (13 ml) was stirred under hydrogen (1 atm) for 16 h and then diluted with EtOAc (15 ml) and filtered through Celite. The filtrate was concentrated *in vacuo* and further dried under high vacuum to give 4-amino-*N*-(2-hydroxyethyl)benzenesulfonamide as a light-brown solid (459 mg, 98%).

Phenylisothiocyanate (180 μl, 1 equivalent) was added to a solution of the above-described crude amine (200 mg, 0.925 mmol) in anhydrous acetonitrile (9 ml). The reaction mixture was stirred at 70°C for 24 h and then concentrated and purified via PTLC (80% EtOAc-hexanes, 2 elutions) to give CF355 (22 mg, 7%) as a white solid (mp of 129.2°C). ^{1}H NMR (400 MHz, CD_3OD) δ 7.83 to 7.78 (m, 2 H), 7.75 to 7.70 (m, 2 H), 7.47 to 7.42 (m, 2 H), 7.40 to 7.34 (m, 2 H), 7.24 to 7.17 (m, 1 H), 3.55 (t, $J = 6.0$ Hz, 2 H), 2.96 (t, $J = 6.0$ Hz, 2 H); ^{13}C NMR (100 MHz, CD_3OD) δ 180.40, 143.37, 138.63, 135.65, 128.52(2), 127.21(2), 125.36, 124.09(2), 122.95(2), 60.40, 44.79.

Quantitative real-time PCR. Strain information is available in Table S1 in the supplemental material. Overnight cultures were diluted 1:100 and grown aerobically in low-glucose Dulbecco's modified Eagle medium (DMEM) (Gibco) for EHEC or in N-minimal medium for *S.* Typhimurium with 5 or 500 nM drug, or with an equivalent volume of dimethyl sulfoxide (DMSO), at 250 rpm to late exponential growth phase (optical density at 600 nm [OD_{600}] = 1.0). RNA was extracted from three biological samples using a RiboPure bacterial RNA isolation kit (Ambion) by following the manufacturer's guidelines. The primers used in the real-time assays were designed using Primer Express v 1.5 (Applied Biosystems) (see Table S2) and were validated for amplification efficiency and template specificity. Quantitative real-time PCR (qRT-PCR) was performed as previously described (17) in a one-step reaction using an ABI 7500 sequence detection system (Applied Biosystems). Data were collected using the ABI Sequence Detection 1.2 software (Applied Biosystems).

All data were normalized to an *rpoA* (RNA polymerase subunit A) endogenous control and analyzed using the comparative critical threshold (C_T) method. Virulence gene expression was presented as fold changes over the expression level of WT EHEC or *S.* Typhimurium grown in the absence of drug. Error bars indicate the standard deviations of the fold change values. The Student unpaired *t* test was used to determine statistical significance.

Fluorescein actin staining. Fluorescein actin staining (FAS) assays were performed as described by Knutton et al. (33). Briefly, HeLa cells were grown on coverslips in 12-well culture plates with DMEM supplemented with 10% fetal bovine serum (FBS) and 1% penicillin-

streptomycin-gentamicin (PSG) antibiotic mix at 37°C and 5% CO_2, overnight to 80% confluence. The wells were washed with phosphate-buffered saline (PBS) and replaced with low-glucose DMEM supplemented with 10% FBS. Bacterial cultures were grown statically overnight in LB in the presence of drug or with an equivalent volume of DMSO at 37°C. Overnight bacterial cultures were diluted 1:100 to infect confluent monolayers of HeLa cells for 6 h at 37°C and 5% CO_2 in the presence or absence of drug. After a 6-h infection, the coverslips were washed, fixed, permeabilized, and then treated with fluorescein isothiocyanate (FITC)-labeled phalloidin to visualize actin accumulation and propidium iodide to visualize host nuclei and bacteria. The coverslips were mounted on slides and visualized with a Zeiss Axiovert microscope. To determine the percentage of infected cells, 5 to 7 fields from three separate coverslips (triplicate) were counted and calculated as follows: (cells with pedestals/total cells) × 100. Statistical analyses were performed using the Student unpaired *t* test.

Mouse survival experiments. For *S.* Typhimurium infections, mice (BALB/c, 7 to 9 weeks old, female) were either treated orally with LED209 (20 mg/kg in 5% DMSO, 23% polyethylene glycol [PEG] 400, 70% sodium bicarbonate [pH 9], 2% Tween 80) at 30 min preinfection only or at 3 h before, at the time of, and 3, 6, 9, and 12 h after infection and then intraperitoneally infected with 10^6 CFU of *S.* Typhimurium strain SL1344. We used 10 mice per treatment, and these experiments were repeated twice to ensure reproducibility. Mice were returned to their cages and monitored daily for signs of morbidity (anorexia, rapid and shallow breathing, scruffy fur, decreased muscle tone, and lethargy) and lethality up to 10 days. The animals that survived were humanely euthanized by CO_2 asphyxiation.

For *F. tularensis* infections, mice (C3H/HeN, female) were either treated orally with LED209 (20 mg/kg in 5% DMSO, 23% PEG 400, 70% sodium bicarbonate [pH 9], 2% Tween 80) at 1, 3, 6, 9, or 24 h prior to infection and then intranasally infected with 30 CFU of *F. tularensis* strain SCHU S4 or intranasally infected with 30 CFU of *F. tularensis* strain SCHU S4 and then treated with LED209 at 1, 3, 6, 9, or 24 h postinfection. All animal work performed with the SCHU S4 strain was conducted in a federally licensed small animal containment level 3. Mice were monitored daily for signs of morbidity and death. At 12 days postinfection, the animals that survived were euthanized by CO_2 asphyxiation.

Macrophage infection. J774 murine macrophages were infected with opsonized *S.* Typhimurium with normal mouse serum at 37°C for 15 min and washed. These macrophages were infected using a multiplicity of infection (MOI) of 100:1 for 30-min bacterium-cell interaction at 37°C and 5% CO_2. These cells were treated with 40 μg/ml of gentamicin for 1 h to kill extracellular bacteria and lysed with 1% Triton-X. Bacteria were diluted and plated in LB plates for CFU determination (34–36). LED209 (5 nM in DMSO) or Om188 (500 nM, 5 nM, or 5 pM) was added to DMEM during the entire incubation.

Biofilm formation inhibition upon LED209 treatment. Biofilm formation was assessed in experiments as previously described (37) and stained by the crystal violet method. All experiments were performed in triplicate using LB broth. Overnight bacterial cultures grown under static conditions were inoculated into fresh medium in a 1:100 dilution on 96-well cell culture polystyrene plates (Falcon). These plates were incubated at 37°C in a CO_2 atmosphere for 24 h. These conditions were assayed in the absence and presence of 5 nM of LED209 (DMSO), and DMSO in the same quantity was employed under all conditions. All these assays were repeated three times to ensure reproducibility.

Clinical isolates. Urine and bladder biopsy samples were isolated from clinically relevant bacterial strains obtained from patients at the UTSW hospitals and clinics under the supervision of Philippe Zimmern. Samples were first enriched in LB broth and isolated in MacConkey agar to differentiate Gram-negative bacteria, as well as lactose fermentation, and classified via API 20E kits, according to the manufacturer's directions (bioMérieux, France).

Construction of *C. rodentium* mutants. Isogenic nonpolar *qseC*, *kdpE*, and *qseBC* mutants were constructed in *C. rodentium* ICC168 using λ-red mutagenesis as previously described (2).

Mouse infection experiments. For mouse survival experiment, 10 3.5-week-old male C3H/HeJ mice per group were infected by oral gavage with either 1×10^9 cells of wild-type *C. rodentium* ICC168 or the Δ*kdpE*, Δ*qseC*, or Δ*qseBC* mutant; five 3.5-week-old male C3H/HeJ mice were inoculated by oral gavage with 100 μl of PBS. Mouse survival in each group was assessed over the course of 14 days.

For bacterial load and colon weight measurement, as well as for colon pathology, 10 3.5-week-old male C3H/HeJ mice per group were infected with 1×10^9 cells of wild-type *C. rodentium* ICC168 or the Δ*kdpE*, Δ*qseC*, or Δ*qseBC* mutant. The infected mice were sacrificed on day 6 postinfection, and their colons were taken. For bacterial load measurement, colons of 5 mice per group were homogenized, and the homogenates were serially diluted and plated on LB agar plates containing 100 μg/ml of nalidixic acid.

Pharmacokinetic analysis. Female CD-1 mice (6 to 7 weeks old) were purchased from Charles River Laboratories. Animals were allowed to acclimate to the animal facility at UT Southwestern Medical Center for approximately 1 week prior to use, and all animal work was approved by the Institutional Animal Care and Use Committee at UT Southwestern. Mice were treated with 5, 20, 80, or 160 mg/kg LED209 given by oral gavage in 10% DMSO, 10% Cremophor EL, 30% PEG 400, and 50% carbonate buffer (pH 10) either a single time or daily for 14 days. At the indicated time points on either day 1 (single dose) or day 14 (chronic dose), animals were given an inhalation overdose of CO_2, and blood was harvested by cardiac puncture with a sodium citrate-coated needle and syringe containing 50 μl of sodium citrate. Plasma was isolated by centrifugation of the blood for 10 min at 9,300 × *g* and frozen at −80°C until analysis. Brains were isolated in an experiment in which animals were dosed at 20 mg/kg, rinsed briefly with PBS to remove surface-adhering blood, weighed, and snap-frozen in liquid nitrogen. Brain homogenates were prepared by homogenizing the brain tissues in a 3-fold volume of PBS (volume of PBS added in milliliters is 3 times the weight of the brain in grams). Total brain homogenate volume was estimated as volume of PBS added plus volume of brain in milliliters. One hundred microliters of plasma or brain homogenate was mixed with 200 μl of acetonitrile containing 0.15% formic acid and 300 ng/ml tolbutamide as an internal standard (IS). The samples were vortexed for 15 s, incubated at room temperature for 10 min, and spun twice at 16,100 × *g* for 5 minutes at 4°C in a standard microcentrifuge to pellet precipitated proteins. Supernatant was collected and samples were analyzed on an ABSciex 4000-Qtrap liquid chromatography-tandem mass spectrometer (LC-MS/MS) in positive MRM mode. The MRM transition monitored for LED209 was 384.0 to 94.1 and 271.2 to 91.2 for the tolbutamide internal standard. A Shimadzu Prominence LC system was used with an Agilent ZORBAX Eclipse XDB-C18 column (5 micron packing, 4.6 × 50 mm). Samples were injected and compound eluted using the following chromatography conditions: buffer A, water and 0.1% formic acid; buffer B, MeOH and 0.1% formic acid; flow rate of 1.5 ml/min; gradient conditions of 0 to 1 min 5% B; 1- to 1.5-min gradient to 95% B; 1.5 to 2.5 min 100% B, 2.5- to 2.6-min gradient to 5% B; 2.6 to 3.5 min 5% B. A standard curve was prepared by using blank murine plasma (Bioreclamation, Westbury, NY) spiked with various concentrations of LED209. The lower limit of detection was set at a signal-to-noise ratio of 3:1 when spiked samples and blank plasma were compared. Standard curves were constructed by plotting the analyte-to-internal standard ratio versus the concentration of LED209 in each sample and a quadratic curve fit to the data using the Analyst software program. A value of three times above the signal obtained in the blank plasma or brain homogenate was designated the limit of detection (LOD). The limit of quantitation (LOQ) was defined as the lowest concentration at which back-calculation yielded a concentration within 20% of the theoretical value and above the LOD signal. The LOQ for LED209 was 1 ng/ml. In general, back-calculation of concentrations indicated the curve was accu-

rate to within 15% over 4 logs from 1,000 to 1 ng/ml. Pharmacokinetic parameters for plasma were determined by using the noncompartmental analysis tool on the WinNonlin software package (Pharsight, Mountain View, CA).

***In vivo* toxicology studies.** Sixteen male and sixteen female CD-1 mice (6 to 7 weeks of age) were purchased from Charles River Laboratories. Animals were allowed to acclimate to the animal facility at UT Southwestern Medical Center for approximately 1 week prior to use, and all animal work was approved by the Institutional Animal Care and Use Committee at UT Southwestern. Animals were placed into one of four groups (vehicle only, 5 mg/kg, 20 mg/kg, or 80 mg/kg) in groups of 4 male and 4 female mice. Animals were dosed daily in the morning by oral gavage with LED209 formulated as 10% DMSO, 10% Cremorphor EL, 30% PEG 400, and 50% carbonate buffer (pH 10) for 14 days. Mice were weighed daily at the same time each day. On day 15, the animals were sacrificed by inhalation overdose of CO_2, blood was collected by cardiac puncture, and organs were isolated and weighed. Whole blood, collected using K_2-EDTA as the anticoagulant, was analyzed by the UT Southwestern Animal Resource Center for complete blood counts. Serum, isolated from whole blood collected in the absence of an anticoagulant, was evaluated by the UTSW Mouse Metabolic Phenotyping Core using the Vitros 250 chemistry analyzer for liver and kidney function. Additionally, a separate sample of serum was shipped to ANI Lytics (Gaithersburg, MD) for measurement of thyroxin (T4) levels as a measure of thyroid function.

hERG radiolabeled ligand binding assay. LED209 was tested at 10 mM in duplicate in a radiolabeled ligand binding assay by MDS Pharma Services (now Eurofins Panlabs, Taipei, Taiwan) for its ability to block the interaction of 1.5 nM astemizole to the hERG channel expressed recombinantly in HEK293 cells. Minimal inhibition (4%) of binding was observed.

SUPPLEMENTAL MATERIAL

Supplemental material for this article may be found at http://mbio.asm.org/lookup/suppl/doi:10.1128/mBio.02165-14/-/DCSupplemental.

Figure S1, PDF file, 0.1 MB.
Figure S2, PDF file, 0.1 MB.
Figure S3, PDF file, 0.1 MB.
Figure S4, PDF file, 0.1 MB.
Table S1, PDF file, 0.03 MB.
Table S2, PDF file, 0.02 MB.
Table S3, PDF file, 0.04 MB.
Table S4, PDF file, 0.04 MB.
Table S5, PDF file, 0.01 MB .
Table S6, PDF file, 0.1 MB.

ACKNOWLEDGMENTS

This work was supported by NIH grants AI077853 and AI053067. M.M.C. was supported through NIH Training Grant 5 T32 AI7520-14.

The contents are solely the responsibility of the authors and do not represent the official views of the NIH NIAID.

REFERENCES

1. **Rasko DA, Sperandio V.** 2010. Anti-virulence strategies to combat bacteria-mediated disease. Nat. Rev. Drug Discov. **9:**117–128. http://dx.doi.org/10.1038/nrd3013.
2. **Petri WA, Jr, Miller M, Binder HJ, Levine MM, Dillingham R, Guerrant RL.** 2008. Enteric infections, diarrhea, and their impact on function and development. J. Clin. Invest. **118:**1277–1290. http://dx.doi.org/10.1172/JCI34005.
3. **Kostakioti M, Hadjifrangiskou M, Cusumano CK, Hannan TJ, Janetka JW, Hultgren SJ.** 2012. Distinguishing the contribution of type 1 pili from that of other QseB-misregulated factors when QseC is absent during urinary tract infection. Infect. Immun. **80:**2826–2834. http://dx.doi.org/10.1128/IAI.00283-12.
4. **Rasko DA, Moreira CG, Li deR, Reading NC, Ritchie JM, Waldor MK, Williams N, Taussig R, Wei S, Roth M, Hughes DT, Huntley JF, Fina MW, Falck JR, Sperandio V.** 2008. Targeting QseC signaling and virulence for antibiotic development. Science **321:**1078–1080. http://dx.doi.org/10.1126/science.1160354.
5. **Moreira CG, Weinshenker D, Sperandio V.** 2010. QseC mediates *Salmonella enterica* serovar Typhimurium virulence *in vitro* and *in vivo*. Infect. Immun. **78:**914–926. http://dx.doi.org/10.1128/IAI.01038-09.
6. **Kostakioti M, Hadjifrangiskou M, Pinkner JS, Hultgren SJ.** 2009. QseC-mediated dephosphorylation of QseB is required for expression of genes associated with virulence in uropathogenic *Escherichia coli*. Mol. Microbiol. **73:**1020–1031. http://dx.doi.org/10.1111/j.1365-2958.2009.06826.x.
7. **Weiss DS, Brotcke A, Henry T, Margolis JJ, Chan K, Monack DM.** 2007. *In vivo* negative selection screen identifies genes required for *Francisella* virulence. Proc. Natl. Acad. Sci. U. S. A. **104:**6037–6042. http://dx.doi.org/10.1073/pnas.0609675104.
8. **Moreira CG, Sperandio V.** 2012. Interplay between the QseC and QseE bacterial adrenergic sensor kinases in *Salmonella enterica* serovar Typhimurium pathogenesis. Infect. Immun. **80:**4344–4353. http://dx.doi.org/10.1128/IAI.00803-12.
9. **Unal CM, Singh B, Fleury C, Singh K, Chávez de Paz L, Svensäter G, Riesbeck K.** 2012. QseC controls biofilm formation of non-typeable *Haemophilus influenzae* in addition to an AI-2-dependent mechanism. Int. J. Med. Microbiol. **302:**261–269. http://dx.doi.org/10.1016/j.ijmm.2012.07.013.
10. **Khajanchi BK, Kozlova EV, Sha J, Popov VL, Chopra AK.** 2012. The two-component QseBC signalling system regulates *in vitro* and *in vivo* virulence of *Aeromonas hydrophila*. Microbiology **158:**259–271. http://dx.doi.org/10.1099/mic.0.051805-0.
11. **Kostakioti M, Hadjifrangiskou M, Cusumano CK, Hannan TJ, Janetka JW, Hultgren SJ.** 2012. Distinguishing the contribution of type 1 pili from that of other QseB-misregulated factors when QseC is absent during urinary tract infection. Infect. Immun. **80:**2826–2834. http://dx.doi.org/10.1128/IAI.00283-12.
12. **Hadjifrangiskou M, Kostakioti M, Chen SL, Henderson JP, Greene SE, Hultgren SJ.** 2011. A central metabolic circuit controlled by QseC in pathogenic *Escherichia coli*. Mol. Microbiol. **80:**1516–1529. http://dx.doi.org/10.1111/j.1365-2958.2011.07660.x.
13. **Novak EA, Shao H, Daep CA, Demuth DR.** 2010. Autoinducer-2 and QseC control biofilm formation and *in vivo* virulence of *Aggregatibacter actinomycetemcomitans*. Infect. Immun. **78:**2919–2926. http://dx.doi.org/10.1128/IAI.01376-09.
14. **Mokrievich AN, Kondakova AN, Valade E, Platonov ME, Vakhrameeva GM, Shaikhutdinova RZ, Mironova RI, Blaha D, Bakhteeva IV, Titareva GM, Kravchenko TB, Kombarova TI, Vidal D, Pavlov VM, Lindner B, Dyatlov IA, Knirel YA.** 2010. Biological properties and structure of the lipopolysaccharide of a vaccine strain of *Francisella tularensis* generated by inactivation of a quorum sensing system gene *qseC*. Biochemistry **75:**443–451. http://dx.doi.org/10.1134/S0006297910040073.
15. **Wang X, Wang Q, Yang M, Xiao J, Liu Q, Wu H.** 2011. QseBC controls flagellar motility, fimbrial hemagglutination and intracellular virulence in fish pathogen *Edwardsiella tarda*. Fish Shellfish Immunol. **30:**944–953. http://dx.doi.org/10.1016/j.fsi.2011.01.019.
16. **Clarke MB, Hughes DT, Zhu C, Boedeker EC, Sperandio V.** 2006. The QseC sensor kinase: a bacterial adrenergic receptor. Proc. Natl. Acad. Sci. U. S. A. **103:**10420–10425. http://dx.doi.org/10.1073/pnas.0604343103.
17. **Hughes DT, Clarke MB, Yamamoto K, Rasko DA, Sperandio V.** 2009. The QseC adrenergic signaling cascade in enterohemorrhagic *E. coli* (EHEC). PLoS Pathog. **5:**e1000553. http://dx.doi.org/10.1371/journal.ppat.1000553.
18. **Clarke MB, Sperandio V.** 2005. Transcriptional regulation of *flhDC* by QseBC and sigma (FliA) in enterohaemorrhagic *Escherichia coli*. Mol. Microbiol. **57:**1734–1749. http://dx.doi.org/10.1111/j.1365-2958.2005.04792.x.
19. **Njoroge JW, Nguyen Y, Curtis MM, Moreira CG, Sperandio V.** 2012. Virulence meets metabolism: *cra* and *kdpE* gene regulation in enterohemorrhagic *Escherichia coli*. mBio **3**(5):e00280-12. http://dx.doi.org/10.1128/mBio.00280-12.
20. **Njoroge J, Sperandio V.** 2012. Enterohemorrhagic *Escherichia coli* virulence regulation by two bacterial adrenergic kinases, QseC and QseE. Infect. Immun. **80:**688–703. http://dx.doi.org/10.1128/IAI.05921-11.
21. **Sperandio V, Torres AG, Kaper JB.** 2002. Quorum sensing *Escherichia coli* regulators B and C (QseBC): a novel two-component regulatory system involved in the regulation of flagella and motility by quorum sensing in *E. coli*. Mol. Microbiol. **43:**809–821. http://dx.doi.org/10.1046/j.1365-2958.2002.02803.x.

22. **Clarke MB, Sperandio V.** 2005. Transcriptional autoregulation by quorum sensing *Escherichia coli* regulators B and C (QseBC) in enterohaemorrhagic *E. coli* (EHEC). Mol. Microbiol. **58:**441–455. http://dx.doi.org/10.1111/j.1365-2958.2005.04819.x.
23. **Reading NC, Torres AG, Kendall MM, Hughes DT, Yamamoto K, Sperandio V.** 2007. A novel two-component signaling system that activates transcription of an enterohemorrhagic *Escherichia coli* effector involved in remodeling of host actin. J. Bacteriol. **189:**2468–2476. http://dx.doi.org/10.1128/JB.01848-06.
24. **Rasko DA, Moreira CG, Li deR, Reading NC, Ritchie JM, Waldor MK, Williams N, Taussig R, Wei S, Roth M, Hughes DT, Huntley JF, Fina MW, Falck JR, Sperandio V.** 2008. Targeting QseC signaling and virulence for antibiotic development. Science **321:**1078–1080. http://dx.doi.org/10.1126/science.1160354.
25. **Reading NC, Rasko DA, Torres AG, Sperandio V.** 2009. The two-component system QseEF and the membrane protein QseG link adrenergic and stress sensing to bacterial pathogenesis. Proc. Natl. Acad. Sci. U. S. A. **106:**5889–5894. http://dx.doi.org/10.1073/pnas.0811409106.
26. **Reading NC, Rasko D, Torres AG, Sperandio V.** 2010. A transcriptome study of the QseEF two-component system and the QseG membrane protein in enterohaemorrhagic *Escherichia coli* O157:H7. Microbiology **156:**1167–1175. http://dx.doi.org/10.1099/mic.0.033027-0.
27. **Pacheco AR, Curtis MM, Ritchie JM, Munera D, Waldor MK, Moreira CG, Sperandio V.** 2012. Fucose sensing regulates bacterial intestinal colonization. Nature **492:**113–117. http://dx.doi.org/10.1038/nature11623.
28. **Kendall MM, Gruber CC, Parker CT, Sperandio V.** 2012. Ethanolamine controls expression of genes encoding components involved in interkingdom signaling and virulence in enterohemorrhagic *Escherichia coli* O157:H7. mBio 3(3):. http://dx.doi.org/10.1128/mBio.00050-12e00050-12.
29. **Gruber CC, Sperandio V.** 2014. Posttranscriptional control of microbe-induced rearrangement of host cell actin. mBio 5(1):e01025-13. http://dx.doi.org/10.1128/mBio.01025-13.
30. **Kostakioti M, Hadjifrangiskou M, Pinkner JS, Hultgren SJ.** 2009. QseC-mediated dephosphorylation of QseB is required for expression of genes associated with virulence in uropathogenic *Escherichia coli*. Mol. Microbiol. **73:**1020–1031. http://dx.doi.org/10.1111/j.1365-2958.2009.06826.x.
31. **Moreira CG, Weinshenker D, Sperandio V.** 2010. QseC mediates *Salmonella enterica* serovar Typhimurium virulence *in vitro* and *in vivo*. Infect. Immun. **78:**914–926. http://dx.doi.org/10.1128/IAI.01038-09.
32. **Rasko DA, Webster DR, Sahl JW, Bashir A, Boisen N, Scheutz F, Paxinos EE, Sebra R, Chin CS, Iliopoulos D, Klammer A, Peluso P, Lee L, Kislyuk AO, Bullard J, Kasarskis A, Wang S, Eid J, Rank D, Redman JC, Steyert SR, Frimodt-Møller J, Struve C, Petersen AM, Krogfelt KA, Nataro JP, Schadt EE, Waldor MK.** 2011. Origins of the *E. coli* strain causing an outbreak of hemolytic-uremic syndrome in Germany. N. Engl. J. Med. **365:**709–717. http://dx.doi.org/10.1056/NEJMoa1106920.
33. **Knutton S, Baldwin T, Williams PH, McNeish AS.** 1989. Actin accumulation at sites of bacterial adhesion to tissue culture cells: basis of a new diagnostic test for enteropathogenic and enterohemorrhagic *Escherichia coli*. Infect. Immun. **57:**1290–1298.
34. **Detweiler CS, Monack DM, Brodsky IE, Mathew H, Falkow S.** 2003. *virK*, *somA* and *rcsC* are important for systemic *Salmonella enterica* serovar Typhimurium infection and cationic peptide resistance. Mol. Microbiol. **48:**385–400. http://dx.doi.org/10.1046/j.1365-2958.2003.03455.x.
35. **Fierer J, Eckmann L, Fang F, Pfeifer C, Finlay BB, Guiney D.** 1993. Expression of the salmonella virulence plasmid gene *spvB* in cultured macrophages and nonphagocytic cells. Infect. Immun. **61:**5231–5236.
36. **Pfeifer CG, Marcus SL, Steele-Mortimer O, Knodler LA, Finlay BB.** 1999. *Salmonella* Typhimurium virulence genes are induced upon bacterial invasion into phagocytic and nonphagocytic cells. Infect. Immun. **67:**5690–5698.
37. **Moreira CG, Palmer K, Whiteley M, Sircili MP, Trabulsi LR, Castro AF, Sperandio V.** 2006. Bundle-forming pili and EspA are involved in biofilm formation by enteropathogenic *Escherichia coli*. J. Bacteriol. **188:**3952–3961. http://dx.doi.org/10.1128/JB.00177-06.